Journal of Hazardous Materials 213–214 (2012) 222–229

Contents lists available at SciVerse ScienceDirect

Journal of Hazardous Materials

journal homepage: www.elsevier.com/locate/jhazmat

Preparation and electrochemical properties of Ce–Ru–SnO_2 ternary oxide anode and electrochemical oxidation of nitrophenols

Yuan Liu[a,b,*], Huiling Liu[a,**], Jun Ma[a], Junjing Li[a]

[a] State Key Laboratory of Urban Water Resources and Environment (SKLUWRE), School of Municipal and Environmental Engineering, Harbin Institute of Technology, Harbin 150090, China

[b] Chongqing Institute of Green and Intelligent Technology, Chinese Academy of Science, Chongqing 401122, China

ARTICLE INFO

Article history:
Received 1 September 2011
Received in revised form
29 December 2011
Accepted 26 January 2012
Available online 6 February 2012

Keywords:
Electrochemical oxidation
Ternary oxides
Tin dioxide
Nitrophenols
Modification

ABSTRACT

A cerium doped ternary SnO_2 based oxides anode that is CeO_2–RuO_2–SnO_2 (Ce–Ru–SnO_2) anode, was prepared by facile thermal decomposition technique. XRD was used to characterize the crystal structures of modified SnO_2 anodes. Electrochemical impedance spectroscopy (EIS) and accelerated life test were also utilized to study the electrochemical property of Ce–Ru–SnO_2 anode. The results indicated that Ce–Ru–SnO_2 anode possessed smaller charge transfer resistance and longer service life than other modified SnO_2 anodes. Oxidants, such as hydroxyl radicals, hydrogen peroxide and hypochlorite ions were determined. Electrochemical oxidation of nitrophenols (NPs) were conducted and compared with previous studies. The degradation of nitrophenols revealed two distinguishing laws for mononitrophenol and multinitrophenols. The Ce–Ru–SnO_2 anode is considered to be a promising material for the treatment of organic pollutants due to its high electrochemical activity and benign stability.

1. Introduction

The increasingly restricted limits for the discharge and disposal of toxic and hazardous materials have required the development of advanced technologies to realize the effective treatment of various wastewaters. Traditional treatment methods, including biological, physical and chemical treatment are ineffective, and thus a number of alternative technologies have been investigated [1]. Electrochemical oxidation as a promising alternative, which can be used for partial or total degradation of these refractory contaminants, has been intensively studied recently [2–4], attributed to its many distinctive advantages including environmental compatibility, versatility, energy efficiency, safety, selectivity, amenability to automation and cost effectiveness.

One of the foremost parts of electrochemical oxidation is obviously the electrode material. The major drawbacks of traditional electrode materials, such as Au, Pt, graphite and glassy carbon, include high cost and low stability, as well as slow degradation rate in the electrochemical oxidation process [5]. Since Beer [6] developed dimensionally stable anodes (DSAs), these have been studied due to their good stability and catalytic activity [7,8]. SnO_2 is one the most widely investigated anode materials for electrochemical oxidation [9,10]. Pure SnO_2 is an *n*-type semiconductor with a band gap of about 3.5 eV and exhibits a very high resistivity at room temperature; thus cannot be used as an electrode material directly [11]. However, its conductivity can be improved significantly by doping antimony, ruthenium, iridium and rare earth elements [10,12,13]. In the electrochemical application, Sb is the most common dopant for SnO_2 due to its low cost and high electrochemical activity [14,15]. However, the major shortcoming of SnO_2–Sb_2O_5 anode is its short lifetime despite the high performance for pollutant oxidation [16]. In the recent years, researchers have made numerous efforts to prolong the life time of SnO_2 based anodes, including (i) addition of additive metal oxides into the coating [17] and (ii) introduction of an interlayer between the substrate and coating [18]. It is well known that the addition of ruthenium and iridium could enhance the life time of SnO_2 based anodes but reduce their electrochemical activity for pollutants elimination.

Rare earth oxides, as powerful oxidants, can catalytically decompose organics readily [19], and have been widely employed as catalysts for oxidation reaction in fuel cell [20]. Recently, some rare earth oxides were introduced into PbO_2 and SnO_2 electrodes to enhance their electrochemical capacities [21,22]. Together with high catalytic activity, CeO_2 is also characteristic of high thermal stability, electrical conductivity and diffusivity [23]. Ceria is a

* Corresponding author at: State Key Laboratory of Urban Water Resources and Environment (SKLUWRE), School of Municipal and Environmental Engineering, Harbin Institute of Technology, Harbin 150090, China. Tel.: +86 23 63063779.
** Corresponding author. Tel.: +86 451 53625118.
E-mail addresses: liuyuan@cigit.ac.cn (Y. Liu), hlliu2002@163.com (H. Liu).

0304-3894/$ – see front matter © 2012 Elsevier B.V. All rights reserved.
doi:10.1016/j.jhazmat.2012.01.090

fluorite oxide, whose cation can switch between +3 and +4 oxidation states. From an experimental point of view, addition of a modulating oxide (e.g. CeO_2) is able to modify the redox level, thus permitting to modulate the electronic properties of electrocatalyst [24]. As discussed in several contributions [25], CeO_2 is a promising candidate to modulate the electrochemical properties of oxide electrodes due to its high Ce(III)/Ce(IV) redox potential. This stimulates us to think that cerium oxide together with ruthenium oxide may be interesting candidate dopants in modification of SnO_2 anode.

Nitrophenols (NPs) are among the most common and versatile industrial organic compounds with extensive application as pesticides, pigments, dyes, pharmaceuticals and explosive materials. These compounds detected in urban and agricultural wastes are anthropogenic, toxic, inhibitory and bio-refractory organic compounds [26] and are considered as hazardous substances and priority toxic pollutants by the United States Environmental Protection Agency (USEPA) [27]. The degradation of NPs by biological treatment is difficult and requires long incubation time since the presence of nitro-group which causes the aromatic compound a strong chemical stability and resistance to microbial degradation [28]. Hence, it is of significant importance to develop new treatment technologies for the decomposition and mineralization of these organic contaminants in wastewater. Up until date, alternative approaches especially advanced oxidation processes (AOPs) have been intensively investigated [29,30]. However, limited number of studies focuses on electrochemical oxidation (ECO), which is one of the most effective AOPs.

The present work aimed to prepare a suitable anode with high performance and long service time for electrochemical oxidation of nitrophenols. A cerium and ruthenium doped ternary SnO_2 based oxide anode (Ce–Ru–SnO_2) was carefully prepared by thermal decomposition technique and examined by means of SEM, XRD and electrochemical impedance spectroscopy (EIS). The electrochemical activity of Ce–Ru–SnO_2 anode was investigated in terms of oxidants yields and degradation of nitrophenols.

2. Experimental

2.1. Materials

High-purity (99.5%) titanium plates with a reaction area of 10 cm^2 (5 cm × 1 cm) were selected as the metal matrix. A stainless steel sheet with the same area as the titanium sheet was used as a cathode. All chemical reagents were analytical grade and used as received without further purification. Solutions were prepared using deionized Milli-Q water.

2.2. Analysis

The crystalline structures of modified SnO_2 anodes were examined using a D/max-rB X-ray diffraction with Cu Kα radiation (λ = 1.5405 Å).

Electrochemical behaviors of modified SnO_2 anodes were tested with a standard three-electrode cell using a computer control potentiostat/galvanostat model 263A (Princeton Applied Research) at room temperature. Modified SnO_2 anodes, a platinum sheet and a saturated calomel electrode were used as working electrode, counter electrode and reference electrode, respectively. The exposed geometric area of the working electrode was 1 cm^2. Electrochemical impedance spectroscopy (EIS) measurements were carried out in 50 mg L^{-1} of *o*-NP as a function of frequency. At a constant potential, the frequencies swept from 100 kHz to 10 mHz with an applied sine wave of 10 mV amplitude. The open-circuit potential was examined in 0.1 M Na_2SO_4 and 0.01 M NaCl mixed aqueous solution.

The stability of modified SnO_2 anodes was tested by means of accelerated life test, which was described as below [31]. The modified SnO_2 anodes, stainless steel sheet and a saturated calomel electrode were used as working electrode, counter electrode and reference electrode, respectively. The test was conducted at a constant anodic current density of 1 A cm^{-2} in the electrolyte of 3 M H_2SO_4, keeping the cell temperature at 298 K. During the test, the variation of potential was measured. In the present work, the span from beginning to inflexion point of the curve cell voltage vs time was defined as the service life of anode.

The oxygen evolution overpotential (OEP) of modified SnO_2 anodes was measured by means of linear sweep in 0.5 M H_2SO_4 at a scan rate of 10 mV S^{-1}. The potentials corresponding to the inflexion point of linear polarization curves were defined as the oxygen evolution overpotential. The detail procedure for determination of OEP could be found elsewhere [21].

The concentration of NPs was measured with a high performance liquid chromatograph. The detail operating parameters could be seen elsewhere [2,32]. The determination of concentration of phenol followed the traditional spectrophotometry. The details about the determination of hydroxyl radicals, hydrogen peroxide and total oxidants could be found elsewhere [32]. The concentration of hypochlorite ion was obtained as difference between the concentration of total oxidants and hydrogen peroxide.

COD was measured by a titrimetric method using dichromate as the oxidant in acidic solution at 458 K for 2 h (Hachi). According to COD, The average current efficiency and specific energy consumption were calculated.

The average current efficiency (ACE, ξ) of each PbO_2 electrode was calculated as the following equation,

$$\zeta = \frac{(COD_0 - COD_t)FV_L}{8I\Delta t 1000} \times 100(\%) \quad (1)$$

where COD_0 and COD_t are the initial and final amount of COD (mg O_2 L^{-1}), F is the Faraday constant (96487 C mol^{-1}), V_L is the volume of electrolyte solution (L), Δt is the degradation time (s), and I is the current intensity (A).

The specific energy consumption (E) of each PbO_2 electrode was also calculated and expressed in the following equation,

$$E = \frac{VI\Delta t}{(COD_0 - COD_t)V_L} (\text{kWh gCOD}^{-1}) \quad (2)$$

where COD_0 and COD_t are the initial and final amount of COD (mg O_2 L^{-1}), V is the average cell potential (V), I is the current (A), and V_L is the volume of electrolyte solution (L).

2.3. Preparation of modified SnO_2 anodes

A set of modified SnO_2 anodes were prepared using the thermal decomposition technique, including SnO_2–Sb_2O_5, SnO_2–RuO_2, Ce–Sb–SnO_2 and Ce–Ru–SnO_2. The pre-treatment of titanium plates could be found in our previous study [33].

As for the preparation of SnO_2–Sb_2O_5 anode, the precursor contained amount of $SnCl_4 \cdot H_2O$ and $SbCl_3$ (molar ratio of Sb/Sn was 1/8) dissolved in 10 mL of 2-proponal–HCl mixture. The precursor was painted onto the pretreated Ti substrates using a brush technique, with excess solvent being evaporated under infrared light at 373 K, followed by calcinations at 823 K for 5 min. These processes were repeated for ten times. A final annealing was then done at 823 K for 1 h within the O_2 atmosphere to complete the fabrication process. With respect to other modified SnO_2 anodes, certain amount of $RuCl_3 \cdot 3H_2O$ and $Ce(NO_3)_3$ were added into the precursors. The subsequent processes were the same as the above. The molar ratios of Ce/Sn and Ru/Sn were 1/100 and 1/10, respectively.

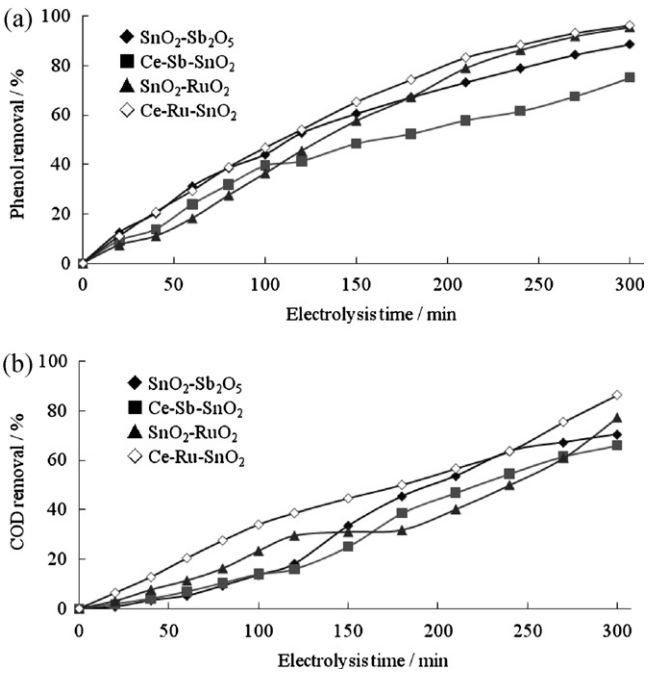

Fig. 1. Variation of phenol removal (a) and COD removal (b) with time on different modified SnO_2 anodes.

2.4. Electrochemical oxidation

The electrochemical oxidation experiments were carried out by batch processes and the apparatus was mainly consisted of a DC power supply, a water bath equipped a magnetic stirrer and a single-compartment glass reactor. The anode (modified SnO_2 anodes) and cathode (stainless steel sheet) were positioned vertically and parallel to each other with a distance of 1 cm.

As for the experiments for investigating the effect of contents of cerium and ruthenium on electrochemical activity of Ce–Ru–SnO_2 anodes, as well electrochemical properties of Ce–Ru–SnO_2 anodes, the conditions included: phenol concentration was 500 mg L^{-1} with volume of 200 mL without pH adjustment, current density was 20 mA cm^{-2}, reaction temperature was 303 K. In order to compare with our previous results, the operating parameters of electrochemical oxidation of NPs were identical to those of our preceding study [33].

3. Results and discussion

3.1. Electrochemical activity of Ce–Ru–SnO_2 anode

The change of phenol removal with electrolysis time on different modified SnO_2 anodes is depicted in Fig. 1a. It can be seen in this figure that Ce–Ru–SnO_2 anode displayed higher phenol degradation efficiency than others. As the electrolysis time reached 300 min, complete elimination of phenol was achieved on Ce–Ru–SnO_2 anode. With respect to SnO_2–RuO_2 anode, more than 95% of phenol was decomposed after 300 min electrolysis. While as for SnO_2–Sb_2O_5 anode, the removal ratio was no more than 88%. Especially, the Ce–Sb–SnO_2 anode demonstrated the worst performance for phenol degradation, only 59% of this compound was decomposed at the end of electrolysis. However, in the first 10 min, one observed that SnO_2–Sb_2O_5 anode displayed a fine electrochemical activity. During this period, the phenol removal of SnO_2–Sb_2O_5 anode was identical to that of Ce–Ru–SnO_2 anode. The possible reason might be ascribed to the fact that as the electrolysis proceeding, the activity of SnO_2–Sb_2O_5 anode decreased gradually,

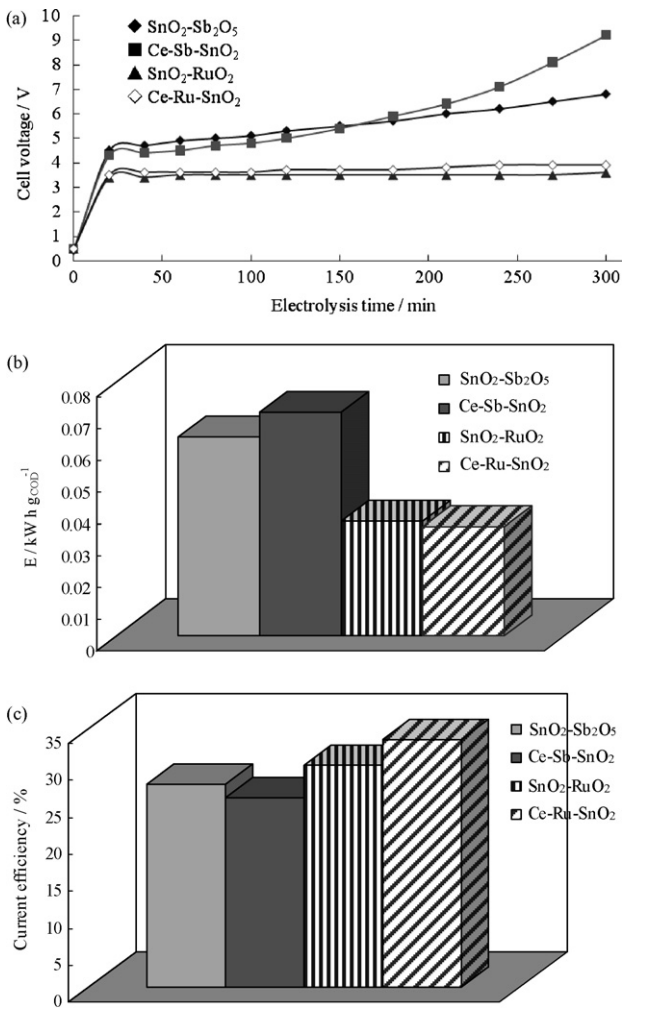

Fig. 2. Variation of cell voltage with time (a), energy consumption (b) and current efficiency (c) of different modified SnO_2 anodes.

which resulted in the gradually increasing discrepancy of removal ratio in comparison with Ce–Ru–SnO_2 anode. As shown in Fig. 1b, the trend of variation of COD removal for each SnO_2 anode was similar to that of phenol mineralization. The final COD removals after 2 h electrolysis for Ce–Ru–SnO_2, SnO_2–RuO_2, SnO_2–Sb_2O_5 and Ce–Sb–SnO_2 anodes were 86%, 77%, 70% and 66%, respectively. The time dependant COD removal of Ce–Ru–SnO_2 anode was higher than others', which was indicative a higher activity of Ce–Ru–SnO_2 anode than others. According to these results, it could elucidate that the incorporation of cerium improved the electrochemical activity of SnO_2–RuO_2 anode, but depressed that of SnO_2–Sb_2O_5 anode.

Fig. 2a presents the variation of cell voltage of these four kinds of modified SnO_2 anodes during electrolysis. The average cell voltages of SnO_2–RuO_2 and Ce–Ru–SnO_2 anodes were lower than those of two others, as depicted in this figure. Furthermore, it also can be seen from this figure that the cell voltages of SnO_2–RuO_2 and Ce–Ru–SnO_2 anodes kept constant in the process of electrolysis, while the cell voltages of SnO_2–Sb_2O_5 and Ce–Sb–SnO_2 anode ascended incessantly. It implied that the stabilities of SnO_2–RuO_2 and Ce–Ru–SnO_2 anodes were superior to that of SnO_2–Sb_2O_5 anode, which was characteristic of short life time as reported in previous studies [34].

On the basis of COD removal and cell voltages, the energy consumption and current efficiency of these four modified SnO_2 anodes were calculated and presented in Fig. 2b and c, respectively. One can see from Fig. 2b that the energy consumptions of SnO_2–RuO_2

Table 1
Oxygen evolution overpotentials of different modified SnO_2 anodes.

	SnO_2–Sb_2O_5	Ce–Sb–SnO_2	SnO_2–RuO_2	Ce–Ru–SnO_2
OEP/V/vs SCE	1.66	1.59	1.60	1.58

and Ce–Ru–SnO_2 anodes were lower. Specifically speaking, if 1 kg of COD was treated, the Ce–Ru–SnO_2 anode would cost 34 kwh of electricity, but SnO_2–Sb_2O_5 anode would cost 62 kwh of electricity. In other words, it would save half of cost by using Ce–Ru–SnO_2 anode for the treatment of wastewater in comparison with SnO_2–Sb_2O_5 anode. In addition, as shown in Fig. 2c that Ce–Ru–SnO_2 anode displayed the highest current efficiency (33.61%) among the four anodes. Therefore, it could be inferred that the Ce–Ru–SnO_2 was a cost effective anode material.

The OEP of these modified SnO_2 anodes were measured and listed in Table 1. The OEP of SnO_2–Sb_2O_5 anode was the highest of all that is 1.66 V (vs SCE), which was in agreement of literature [35]. However, the OEPs of other modified anodes were somewhat lower. The OEPs of Ce–Sb–SnO_2, SnO_2–RuO_2 and Ce–Ru–SnO_2 anodes were 1.59 V, 1.60 V and 1.58 V (vs SCE), respectively. In spite of the lower OEP of Ce–Ru–SnO_2 anode, its phenol removal was better than that of SnO_2–Sb_2O_5 (as shown in Fig. 1). The possible reason may be as follows. In the course of galvanostatic electrolysis, the cell voltage was associated with the potential of electrodes and electrolyte resistance. The cell voltage could be simply described as the following equation: $E_{cell} = E_{theo} + E_{over} + E_{system}$, where E_{cell} is the cell voltage, E_{theo} is the theoretic electrolysis potential, E_{over} is the summary of overpotential of anode and cathode and E_{system} is the summary of voltage loss deriving from electrolyte resistance and wire resistance. With regard to the same electrochemical cell, the theoretic electrolysis potential, electrolyte resistance and wire resistance showed negligible difference among different modified SnO_2 used as anodes. Therefore, the different value of cell voltage originated from the different overpotential. Due to the same cathode used and same cathodic reaction took place, the cathodic overpotential was considered as a constant among the four electrolysis systems where different anodes were used. Consequently, the different overpotential was from the different anodic overpotential, which also implied that the different cell voltage was resulted from the difference anodic overpotential. The cell voltage of SnO_2–Sb_2O_5 anode was higher than that of Ce–Ru–SnO_2, herein, the overpotential of SnO_2–Sb_2O_5 anode was also higher than that of Ce–Ru–SnO_2. The value of anodic overpotential was related to the extent of oxygen evolution. The larger the anodic overpotential was, the more violent the oxygen evolution reaction would take place, which was a competing reaction for organics oxidation and depressed the phenol electrochemical oxidation. The smaller cell voltage observed when Ce–Ru–SnO_2 was used as anode resulted in lower anodic overpotential, which was in favor of the electrochemical oxidation of phenol. Therefore, it could be the reason for why the OEP of Ce–Ru–SnO_2 anode was lower but the phenol removal efficiency was higher than SnO_2–Sb_2O_5 anode.

By the way, according to the above results, Ce–Sb–SnO_2 anode was no longer under consideration in the subsequent studies.

3.2. Crystal structures of Ce–Ru–SnO_2 anode

Fig. 3 presents the XRD patterns of the modified SnO_2 anodes. The diffraction peaks revealed that SnO_2 was in the form of tetrahedral crystalline. According to the XRD patterns of SnO_2–RuO_2 and Ce–Ru–SnO_2 anodes, the diffraction peaks corresponding to RuO_2 and CeO_2 were observed, which indicated that ruthenium and cerium existed in the form of their oxides by the present preparation technique. The crystal sizes of modified SnO_2 anodes were

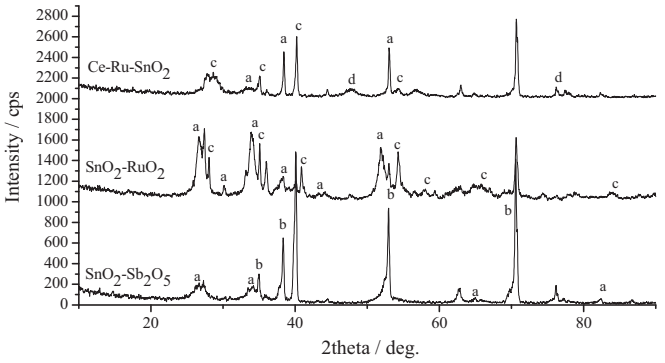

Fig. 3. X-ray diffraction patterns of modified SnO_2 anodes: (a) SnO_2; (b) Sb_2O_5; (c) RuO_2; (d) CeO_2.

Table 2
Crystal sizes of modified SnO_2 anodes.

Modified SnO_2 anodes	Crystal size (nm)
Ti/SnO_2–Sb_2O_5	25.0347
Ti/SnO_2–RuO_2	23.2659
Ti/Ce–Ru–SnO_2	19.3669

calculated with Scherrer's formula are presented in Table 2. The result suggested that the incorporation of cerium could diminish the size of crystals, which in turn was in favor of increasing the specific surface area of Ce–Ru–SnO_2 anode. According to the result of literature [24], the different structure between CeO_2 (cubic) and SnO_2 and RuO_2 (rutile) would result in a smaller crystal size and higher dispersion of oxides thus increasing the electrochemically active surface area. As we know, the electrochemical activity of anode is related to its specific surface area. Consequently, the better electrochemical activity of Ce–Ru–SnO_2 anode was probably due to its high specific surface area. Therefore, these would be attributed to the higher electrochemical activity of Ce–Ru–SnO_2 anode.

3.3. Electrochemical measurements of Ce–Ru–SnO_2 anode

Fig. 4 presents the results of accelerated life tests of modified SnO_2 anodes. It can be seen from this figure that the service life of SnO_2–Sb_2O_5 anode was considerably short, i.e. 1.42 h, which was in agreement with the results of previous studies [16]. Contrarily, the service lives of ruthenium doped SnO_2 anodes were 318 h and 340 h for SnO_2–RuO_2 and Ce–Ru–SnO_2 anodes, respectively. It implied that the incorporation of ruthenium was able to prolong the lifetime of anodes, which was consistent of literatures [12]. What is more, the service life of Ce–Ru–SnO_2 anode was even higher than that of SnO_2–RuO_2 anode. It might be ascribed to the reason that

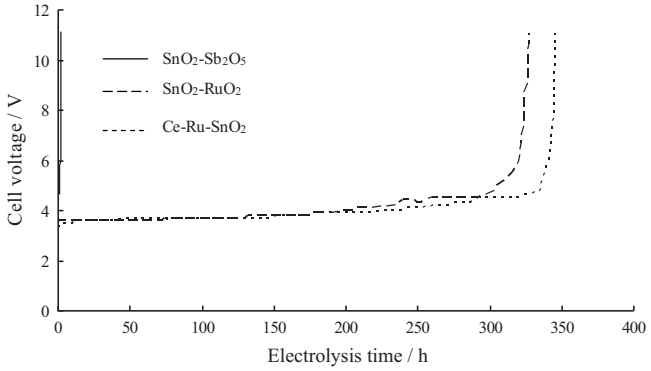

Fig. 4. Accelerated life tests of modified SnO_2 anodes.

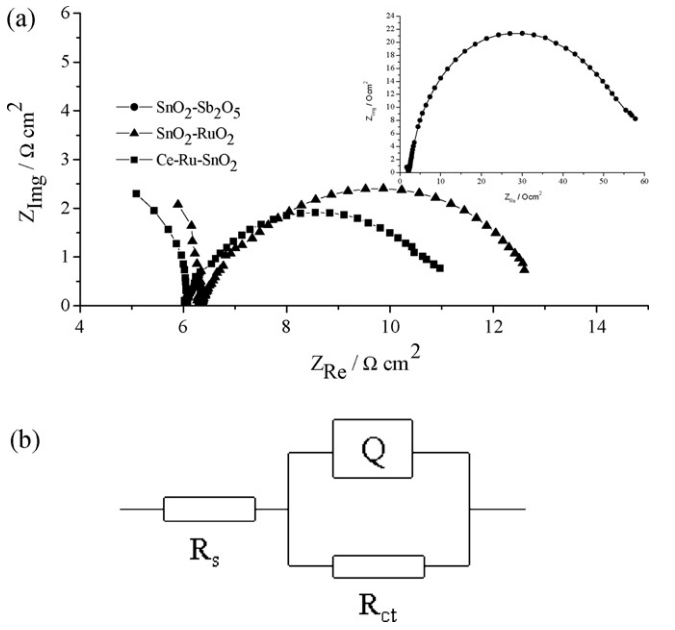

Fig. 5. Results of EIS (a) and equivalent circuit (b) of modified SnO_2 anodes, constant potential: SnO_2–Sb_2O_5, 1.55 V (vs SCE), SnO_2–RuO_2, 1.45 V (vs SCE) and Ce–Ru–SnO_2, 1.4 V (vs SCE).

compound like solid solution was formed in the course of annealing of cerium, tin and ruthenium. It further formed a layer of compact protective film on the surface of anode, which was able to alleviate the occurrence of corrosion, so as to enhance the capacity of anti-corrosion of anode. The results of open-circuit potentials of SnO_2–Sb_2O_5, SnO_2-RuO_2 and Ce–Ru–SnO_2 anodes were 0.06, 0.11 and 0.16 V (vs SCE, data not shown), respectively. It also indicated that the incorporation of cerium indeed improved the capacity of anti-corrosion of anode.

EIS studies were employed for further investigation of electrochemical properties of modified SnO_2 anodes. Fig. 5a presents the Nyquist plots for these anodes. In this figure, three well-defined capacitance arcs for each anode were observed, which suggested that reaction took place at its constant potential. As shown in Fig. 5a, the plots displayed a semicircle patterns covered the midfrequency and low frequency regions, which implied that mass diffusion control was negligible in the present systems. As we know, all the OEPs were above the constant potentials, so that the reaction might include the direct oxidation of organic compound and/or discharge of water. EIS simulation results were obtained by fitting of experimental data using an equivalent circuit model described by Adams et al. [17] as shown in Fig. 5b. In this circuit, R_s presents the solution resistance, Q is the constant phase element (CPE) for double-layer, and R_{ct} is the charge transfer resistance, respectively. The simulation parameters of EIS data are listed in Table 3. The values of Q were all in the range of 0.8–1.0 indicating that the CPE component was close to a pure capacitor for all the anodes. The charge transfer resistance decreased in the order of: SnO_2–Sb_2O_5 (55.88 Ω cm^2) > SnO_2–RuO_2 (6.623 Ω cm^2) > Ce–Ru–SnO_2 (5.095 Ω cm^2). This indicated that the transfer of electrons was easier on the Ce–Ru–SnO_2 anode, so that this anode possessed higher electrochemical activity [34]. Combing with the results presented in Table 1 and Fig. 2a, the results of EIS indicated that despite of the slight lower OEP of Ce–Ru–SnO_2 than SnO_2–Sb_2O_5, the significantly smaller charge transfer resistance of the former still guaranteed its superior electrochemical activity to the latter.

Table 3
EIS simulating parameters of modified SnO_2 anodes.

	R_s (Ω cm^2)	R_{ct} (Ω cm^2)	CPE (mF cm^2)	n
Ti/SnO_2–Sb_2O_5	6.136	55.88	2.632	0.8533
Ti/SnO_2–RuO_2	6.335	6.623	19.42	0.8055
Ti/Ce–Ru–SnO_2	6.056	5.095	31.13	0.8281

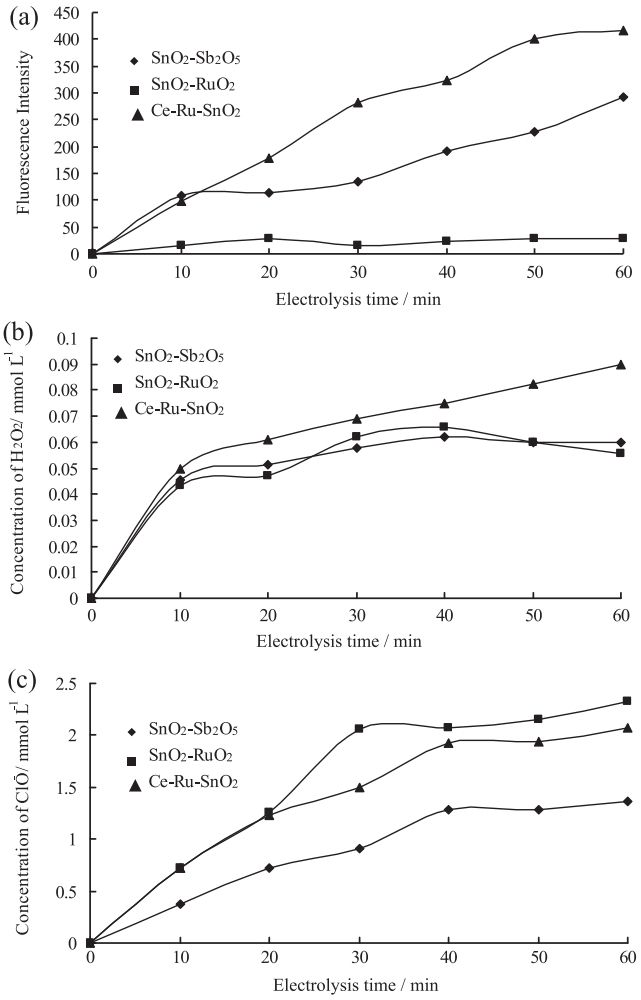

Fig. 6. Trends of fluorescence intensity (a), concentration of H_2O_2 (b), concentration hypochlorite ion (c) with time on modified SnO_2 anodes.

3.4. Oxidants analysis

According to our previous study [33], the yield of oxidants would indirectly reflect the electrochemical activity of electrodes. The evolutions of concentrations of oxidants are presented in Fig. 6. Above all, as shown in Fig. 6a, the yield of hydroxyl radicals of SnO_2–RuO_2 anode was much less than that of two other anodes, which might be due to the intrinsic nature of RuO_2. This oxide has been widely investigated as the catalyst for oxygen or chlorine production for a long time [36]. Incorporation of this oxide into the film of SnO_2 anode would enhance the evolution of oxygen or chlorine, resulting in decreasing the generation of hydroxyl radicals. The result presented in Fig. 6c also confirmed that SnO_2–RuO_2 anode was in favor of the formation of chlorine, because one of the ways corresponding to the formation of hypochlorite ions was the hydrolyzation of chlorine. Therefore, an indirect implication for easier evolution of chlorine on SnO_2–RuO_2 anode than other anodes was illustrated in terms of these data. The similar phenol mineralization of SnO_2–RuO_2 anode to Ce–Ru–SnO_2 anodes observed in

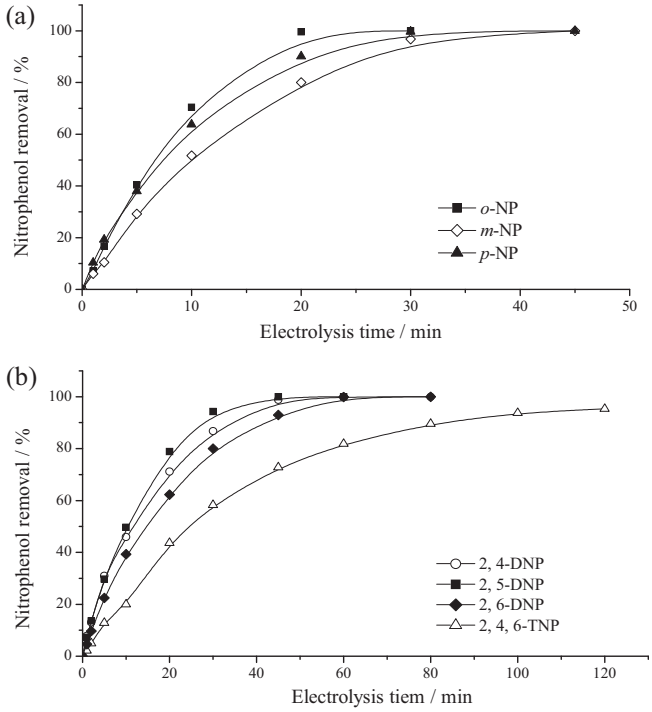

Fig. 7. Variations of NPs removal as a function of electrolysis time at Ce–Sb–SnO_2 anodes: (a) mononitrphenols; (b) multinitrophenols.

Fig. 1 was due to fact that phenol was decomposed by hypochlorite ion, which was also a strong oxidative species and able to decompose organic compounds, generated on SnO_2–RuO_2 anode. Therefore, despite of the low concentration of hydroxyl radicals of SnO_2–RuO_2 anode, the higher amount of hypochlorite ion also verified its similar electrochemical activity to that of Ce–Ru–SnO_2 anode.

On the other hand, ruthenium was also doped into Ce–Ru–SnO_2 anode, but this anode displayed the largest yield of hydroxyl radicals of all the modified SnO_2 anodes. This result suggested that the incorporation of cerium resulted in a great enhancement of electrochemical activity of SnO_2–RuO_2 anode. Cerium played the role of active centers on Ce–Ru–SnO_2 anode, so that the number of active sites, which could adsorb water and cause them discharge to form hydroxyl radicals was increased. It was probable that cerium and ruthenium played different roles on Ce–Ru–SnO_2 anode. The former was able to improve the electrochemical activity, and the latter facilitated the enhancement of stability of anode. In addition, the amounts of both hydrogen peroxide and hypochlorite ions of Ce–Ru–SnO_2 anode were higher, which also indicated the outperformed electrochemical performance for this anode.

3.5. Electrochemical oxidation of nitrophenols on Ce–Ru–SnO_2 anode

The Ce–Ru–SnO_2 anode was used for the electrochemical oxidation of nitrophenols, and the results were presented in Fig. 7. It can be seen from this figure that all the nitrophenols except 2,4,6-TNP were completely decomposed at the end of electrolysis. The regression analysis of the concentration curves versus reaction time indicated that the decay of these NPs could also be described by the pseudo-first order kinetics formula with respect to NP concentration: $dC_{NP}/dt = -C_{NP}$. The pseudo-first-order rate constants listed in Table 4 suggest that the degradation of NPs lies in the order:

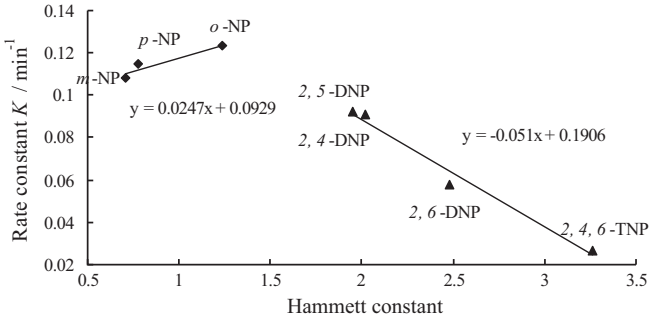

Fig. 8. Relationship between rate constant k and Hammett's constant (σ) of NPs at Ce–Sb–SnO_2 anodes.

o-NP > *p*-NP > *m*-NP > 2,5-DNP > 2,4-DNP > 2,6-DNP > 2,4,6-TNP. In the view of global reaction rates, the degradation of NPs is in the order: mononitrophenols > dinitrophenols > trinitrophenols, which is consistent of the results of Ti/Bi–PbO_2 anode [2,32]. This result revealed a law that if the kinds of substituents on the aromatic rings are identical, larger number of substituents would result in smaller degradation rates.

On the basis of previous studies [32,37], nitro-group has been testified to have effect on properties of NPs in terms of its number and position on aromatic rings. The Hammett constant represents the effect that the various substituents have on the electronic character of a given aromatic system [38]. Hammett constant (σ) of multi-substituted nitrophenol (shown in Table 4) was calculated as a sum of σ's of nitro groups, adopting the values 0.71, 0.78 and 1.24, respectively, for *meta*-, *para*- and *ortho*-positions [39]. The larger value corresponded to stronger electron-withdrawing capacity of groups. Some researchers concluded that the degradation phenolic compounds followed the law of Hammett constant, i.e. the degradation rate had a linear relationship with the value of Hammett constant. Ksibi et al. [40] reported their investigation on the relationship between Hammett constant and the degradation of three NPs with different number of nitro-group on aromatic rings. They pointed out that the smaller the Hammett constant was, the faster the compounds were decomposed. In other words, the more the number of substituent was, the more difficult it could be oxidized. Zhu et al. [37] also studied the relationship between Hammett constant and the nature of *p*-substituted phenols with different kinds of substituents. They came out an opposite conclusion that the degradation rate of *p*-substituted phenols raised with an increase of Hammett constants.

However, in the present work, as shown in Fig. 8 and Table 4, two distinctive laws about the relationship between rate constants of NPs and Hammett constant were observed. On one hand, with respect to mononitrophenols, the result of the present work was in agreement with other literatures [29], that is the larger the Hammett constant was, the faster the degradation rate of NPs was. Hydroxyl radical is characteristic of strong electrophilic, and attacks those groups or carbon atom of the aromatic ring with high electron

Table 4
Pseudo-first-order rate constants k of NPs as well as their Hammett constants (σ).

NPs	k (min^{-1})	Correlation coefficient R^2	σ
o-NP	0.1232	0.9937	1.24
m-NP	0.1083	0.9622	0.71
p-NP	0.1146	0.9952	0.78
2,4-DNP	0.0908	0.9476	2.02
2,5-DNP	0.0921	0.9830	1.95
2,6-DNP	0.0576	0.9934	2.48
2,4,6-TNP	0.0269	0.9954	3.26

density preferentially. The electron-donating substituent, phenolic —OH group, increase the electron density at *ortho* and *para* positions, while electron-withdrawing substituent, —NO_2 group, is strongly deactivating the *meta* position. When both these substituents (—OH and -NO_2) are present, the electrophilic attack will occur preferentially at *ortho* and *para* positions. In addition, due to the existence of electron-withdrawing substituent, i.e. —NO_2 group, the reducibility of aromatic rings was reinforced. Therefore, the larger Hammett constant would result in a greater reducibility of aromatic ring. As a result, the compound was more readily to be attacked by hydroxyl radicals. Consequently, it inferred that the attack and substitution towards hydrogen atoms on aromatic rings by hydroxyl radicals should be involved in the first stage of electrochemical oxidation of mononitrophenols on Ce–Ru–SnO_2 anode.

On the other hand, with respect to multinitrophenols, a different degradation law between the rate constants and Hammett constants was revealed as depicted in Fig. 8. This result was completely contrary to that of mononitrophenols, but in agreement with previous study [40]. Besides the substitution towards hydrogen atom on the aromatic rings by hydroxyl radical, there ought to be another possible reaction, i.e. the substitution of nitro groups, in the course of the attack of hydroxyl radicals to aromatic rings. As a consequence, the reaction took place preferentially at those positions with higher electron density, including nitro groups, *ortho* and *para* positions of aromatic rings. The steric effect should be taken into consideration that it might play an important role in the course of the attack of hydroxyl radicals to aromatic rings. For instance, as for the molecular structure of 2,6-DNP, both nitro groups were on the two *ortho* positions of aromatic ring and aside phenolic hydroxyl group. Therefore, it was difficult for hydroxyl radicals to attack these nitro groups, whereas the *para* position of aromatic ring. With respect to the structure of 2,5-DNP, hydrogen atoms on *ortho* and *para* positions and nitro group on *meta* position would be readily attacked by hydroxyl radicals. While for 2,4-DNP, hydrogen atom on *ortho* position and nitro group on *para* position were under the potential attack by hydroxyl radicals. As for 2,4,6-TNP, it has the largest steric resistance due to its complex molecular structure, so that it was hard to be decomposed. Generally speaking, the substitution of hydrogen atoms and nitro groups on aromatic rings by hydroxyl radicals should be involved in the initial stage of electrochemical oxidation of multinitrophenols on Ce–Ru–SnO_2 anode.

4. Conclusions

The result of XRD revealed that the incorporation of cerium could diminish the crystal size of modified SnO_2 anode. The results of accelerated life test indicated that the service life of Ce–Ru–SnO_2 anode was longer than that of traditional SnO_2–Sb_2O_5 anode. The result of EIS suggested that Ce–Ru–SnO_2 anode had smaller charge transfer resistance than others, which indicated that electrons were believed to transfer more readily on the Ce–Ru–SnO_2 anode. The amount of hydroxyl radicals generated on Ce–Ru–SnO_2 anode was larger than that of other modified SnO_2 anodes, indicating that Ce–Ru–SnO_2 anode has a higher electrochemical activity. Nitrophenols could be effectively eliminated on Ce–Ru–SnO_2 anode. The degradation of NPs lies in the order: *o*-NP > *p*-NP > *m*-NP > 2,5-DNP > 2,4-DNP > 2,6-DNP > 2,4,6-TNP. The relationship between rate constants of nitrophenols and their Hammett constants revealed two distinguishing laws for monnitrophenols and multinitrophenols. Therefore, the Ce–Ru–SnO_2 anode is considered to be a promising material for the treatment of organic pollutants due to its high electrochemical activity and benign stability.

Acknowledgment

This work was supported by National Natural Science Foundation of China (No. 51178138), National Creative Research Groups of National Natural Science Foundation of China (No. 51121062).

References

[1] C. Wang, J. Li, G. Mele, G.M. Yang, F.X. Zhang, L. Palmisano, G. Vasapollo, Efficient degradation of 4-nitrophenol by using functionalized porphyrin-TiO_2 photocatalysts under visible irradiation, Appl. Catal. B: Environ. 76 (2007) 218–226.
[2] Y. Liu, H.L. Liu, Y. Li, Comparative study of the electrocatalytic oxidation and mechanism of nitrophenols at Bi-doped lead dioxide anodes, Appl. Catal. B: Environ. 84 (2008) 297–302.
[3] B. Nasr, G. Abdellatif, P. Cañizares, C. Sáez, M.A. Rodrigo, Electrochemical oxidation of hydroquinone, resorcinol, and catechol on boron-doped diamond anodes, Environ. Sci. Technol. 39 (2005) 7234–7239.
[4] C.R. Costa, F. Montilla, E. Morallón, P. Olivi, Electrochemical oxidation of synthetic tannery wastewater in chloride-free aqueous media, J. Hazard. Mater. 180 (2010) 429–435.
[5] D.C. Johnson, J. Feng, L.L. Houk, Direct electrochemical degradation of organic wastes in aqueous media, Electrochim. Acta 46 (2000) 323–330.
[6] H.B. Beer, US Patent 3632498, 1976.
[7] M. Panizza, G. Cerisola, Electrocatalytic materials for the electrochemical oxidation of synthetic dyes, Appl. Catal. B: Environ. 75 (2007) 95–101.
[8] Y.J. Feng, Y.H. Cui, B. Logan, Z.Q. Liu, Performance of Gd-doped Ti-based Sb–SnO_2 anodes for electrochemical destruction of phenol, Chemosphere 70 (2008) 1629–1636.
[9] C. Comninellis, C. Pulgarin, Electrochemical oxidation of phenol for wastewater treatment using SnO_2 anodes, J. Appl. Electrochem. 23 (1993) 108–112.
[10] M.E. Makgae, M.J. Klink, A.M. Crouch, Performance of sol–gel titanium mixed metal oxide electrodes for electro-catalytic oxidation of phenol, Appl. Catal. B: Environ. 84 (2008) 659–666.
[11] G.H. Chen, Electrochemical technologies in wastewater treatment, Sep. Purif. Technol. 38 (2004) 11–41.
[12] L.V. Gomez, S. Ferro, A. De Battisti, Preparation and characterization of RuO_2–IrO_2–SnO_2 ternary mixtures for advanced electrochemical technology, Appl. Catal. B: Environ. 67 (2006) 34–40.
[13] C.C. Hu, K.H. Chang, C.C. Wang, Two-step hydrothermal synthesis of Ru–Sn oxide composites for electrochemical supercapacitors, Electrochim. Acta 52 (2007) 4411–4418.
[14] R. Cossu, A.M. Polcaro, M.C. Lavagnolo, M. Mascia, S. Palmas, F. Renoldi, Electrochemical treatment of landfill leachate: oxidation at Ti/PbO_2 and Ti/SnO_2 anodes, Environ. Sci. Technol. 32 (1998) 3570–3573.
[15] C. Borras, C. Berzoy, J. Mostany, J.C. Herrera, B.R. Scharifker, A comparison of the electrooxidation kinetics of *p*-methoxyphenol and *p*-nitrophenol on Sb-doped SnO_2 surfaces: concentration and temperature effects, Appl. Catal. B: Environ. 72 (2007) 98–104.
[16] R.J. Watts, M.S. Wyeth, D.D. Finn, A.L. Teel, Optimization of Ti/SnO_2–Sb_2O_5 anode preparation for electrochemical oxidation of organic contaminants in water and wastewater, J. Appl. Electrochem. 38 (2008) 31–37.
[17] B. Adams, M. Tian, A.C. Chen, Design and electrochemical study of SnO_2-based mixed oxide electrodes, Electrochim. Acta 54 (2009) 1491–1498.
[18] B. Wang, W.P. Kong, H.Z. Ma, Electrochemical treatment of paper mill wastewater using three-dimensional electrodes with Ti/Co/SnO_2–Sb_2O_5 anode, J. Hazard. Mater. 146 (2007) 295–301.
[19] S.Y. Ai, M.N. Gao, W. Zhang, Q.J. Wang, Y.F. Xie, L.T. Jin, Preparation of Ce–PbO_2 modified electrode and its application in detection of anilines, Talanta 62 (2004) 445–450.
[20] Z.C. Tang, G.X. Lu, High performance rare earth oxides LnO(x) (Ln = Sc, Y, La, Ce, Pr and Nd) modified Pt/C electrocatalysts for methanol electrooxidation, J. Power Sources 162 (2006) 1067–1072.
[21] Y. Liu, H.L. Liu, J. Ma, J.J Li, Investigation on electrochemical properties of cerium doped lead dioxide anode and application for elimination of nitro-phenol, Electrochim. Acta 56 (2011) 1352–1360.
[22] Y.H. Song, G. Wei, R.C. Xiong, Structure and properties of PbO_2–CeO_2 anodes on stainless steel, Electrochim. Acta 52 (2007) 7022–7027.
[23] D.E. Zhang, X.M. Ni, H.G. Zheng, X.J. Zhang, J.M. Song, Fabrication of rod-like CeO_2: characterization, optical and electrochemical properties, Solid State Sci. 8 (2006) 1290–1293.
[24] K.C. Fernandes, L.M. Da Silva, J.F.C. Boodts, L.A. De Faria, Surface, kinetics and electrocatalytic properties of the Ti/Ti + Ru + Ce)O-2-system for the oxygen evolution reaction in alkaline medium, Electrochim. Acta 51 (2006) 2809–2818.
[25] L.M. Da Silva, K.C. Fernandes, L.A. De Faria, J.F.C. Boodts, Electrochemical impedance spectroscopy study during accelerated life test of conductive oxides: Ti/(Ru + Ti + Ce)O^{-2}-system, Electrochim. Acta 49 (2004) 4893–4906.
[26] R. Belloli, E. Bolzacchini, L. Clerici, B. Rindone, G. Sesana, V. Librando, Nitrophenols in air and rainwater, Environ. Eng. Sci. 23 (2006) 405–415.
[27] USEPA, Environmental Protection Agency, Environmental Criteria, Assessment Office. Cicinnati, OH: US, 1985.
[28] S. Yi, W.Q. Zhuang, B. Wu, S.T.L. Tay, J.H. Tay, Biodegradation of *p*-nitrophenol by aerobic granules in a sequencing batch reactor, Environ. Sci. Technol. 40 (2006) 2396–2401.

[29] V. Kavitha, K. Palanivelu, Degradation of nitrophenols by Fenton and photo-Fenton processes, J. Photochem. Photobiol. A: Chem. 170 (2005) 83–95.
[30] A. Goi, M. Trapido, T.A. Tuhkanen, A study of toxicity, biodegradability, and some by-products of ozonized nitrophenols, Adv. Environ. Res. 8 (2004) 303–311.
[31] X.M. Chen, G.H. Chen, P.L. Yue, Stable Ti/IrO_x–Sb_2O_5–SnO_2 anode for O^{-2} evolution with low Ir content, J. Phys. Chem. B 105 (2001) 4623–4628.
[32] Y. Liu, H.L. Liu, J. Ma, X. Wang, Comparison of degradation mechanism of electrochemical oxidation of di- and tri- nitrophenols on bi-doped lead dioxide electrode: effect of the molecular structure, Appl. Catal. B: Environ. 91 (2009) 284–299.
[33] Y. Liu, H.L. Liu, Comparative studies on the electrocatalytic properties of modified PbO_2 anodes, Electrochim. Acta 53 (2008) 5077–5083.
[34] X.M. Chen, F.R. Gao, G.H. Chen, Comparison of Ti/BDD and Ti/SnO_2–Sb_2O_5 electrodes for pollutant oxidation, J. Appl. Electrochem. 35 (2005) 185–191.
[35] B. Correa-Lozano, Ch Comninellis, A.D. Battisti, Preparation of SnO_2–Sb_2O_5 films by the spray pyrolysis technique, J. Appl. Electrochem. 26 (1996) 83–89.
[36] V. Dharuman, K.C. Pillai, RuO_2 electrode surface effects in electrocatalytic oxidation of glucose, J. Solid State Electrochem. 10 (2006) 967–979.
[37] X.P. Zhu, S.Y. Shi, J.J. Wei, F.X. Lv, H.Z. Zhao, J.T. Kong, Q. He, J.R. Ni, Electrochemical oxidation characteristics of *p*-substituted phenols using a boron-doped diamond electrode, Environ. Sci. Technol. 41 (2007) 6541–6546.
[38] J.A. Dean, Handbook of Organic Chemistry, McGraw-Hill, New York, 1987.
[39] M.B. Smith, J. March, Advanced Organic Chemistry, 5th ed., Wiley, New York, 2001.
[40] M. Ksibi, A. Zemzemi, R. Boukchina, Photocatalytic degradability of substituted phenols over UV irradiated TiO_2, J. Photochem. Photobiol. A: Chem. 159 (2003) 61–70.